

## New Insights into the Photoreactivity of the Organophosphorus Pesticide Fenthion: A $\sigma$ Aryl Cation as a Key Intermediate in the Photodecomposition

STEFANO TORRISI AND SALVATORE SORTINO\*

Dipartimento di Scienze Chimiche, Università di Catania, I-95125 Catania, Italy

The primary photodegradation processes of fenthion (FN), one of the most photosensitive pesticides used in agriculture, have been investigated by combining laser flash photolysis and steady-state measurements. The triplet state of FN is produced quite efficiently ( $\Phi_{isc} \sim 0.3$ ). However, this excited state does not seem to trigger the primary photodecomposition pathways of the pesticide. It is demonstrated that FN undergoes photoheterolysis via the excited singlet state and gives the corresponding *singlet* " $\sigma$  aryl cation". Chemical evidence for the generation of this transient species is given by trapping with typical " $\sigma$  nucleophiles" such as chloride and methanol. This photodegradation mechanism is, in part, quite different with respect to what is known to date and may account for the formation of the *O,O*-dimethyl *S*-[3-methyl-4-(methylthio)phenyl] phosphorothioate discovered as a novel photodegradation product of FN.

**KEYWORDS:** Fenthion; pesticide; photodegradation; aryl cation; laser flash photolysis

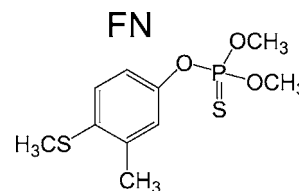
### INTRODUCTION

Organophosphorus pesticides are widely used in modern agriculture as an alternative to organochlorines for pest control. This common class of compounds represents more than one-third of the total insecticides used in the world (1) and acts via inhibition of the enzyme cholinesterase, which plays a key role in the insect's nervous system (2).

Among factors affecting the persistence of pesticide in the environment (i.e., oxidation, metabolism in plants and animals, bacteriological degradation, hydrolysis) (3–6) photolysis is one of the foremost. In this regard, an increasing number of papers devoted to the photodegradation of pesticides has appeared in the literature in recent years (7). The importance of these studies is manifold. For example, light-mediated processes provide an interesting route for effective treatment of pesticide-polluted ground and surface waters. Moreover, because pesticides themselves and/or their degradation products may be ingested by humans with agricultural products, elucidation of the photodegradation pathways is of relevance in view of the potential toxic and phototoxic effects on human health. Finally, this subject may be of fundamental photochemical interest as far as aspects strictly connected to the mechanisms of photo-initiated reactions are concerned.

Fenthion (FN), *O,O*-dimethyl *O*-[3-methyl-4-(methylthio)phenyl] phosphorothioate (**Chart 1**), is an organophosphorus insecticide recently come to the limelight because of its remarkably high photosensitivity. Actually, a recent investigation by Hirahara et al. demonstrated that FN is the most photosensi-

Chart 1



tive among 79 pesticides including organophosphorus, organo-nitrogen, organochlorine, and pyrethroid compounds (8). The same authors contributed to the understanding of the photodegradation of FN by identifying three main aromatic photo-products (9, 10).

Two different pathways have been proposed to play a dominant role in the FN photolysis: (i) photochemical hydrolysis involving nucleophilic attack of water to the P atom and subsequent cleavage of the O–P bond and (ii) a photo-oxidative route mediated by singlet oxygen (9). However, to draw a more detailed picture of the photodegradation mechanism of this pesticide, further points still need to be clarified.

To this aim we have undertaken an investigation combining laser flash photolysis and steady-state measurements. It is shown that new insights have been gained on both excited states and key intermediates involved in FN photodecomposition.

### MATERIALS AND METHODS

**Chemicals.** FN was purchased from Supelco (St. Louis MO) with a purity grade of 98% and was further purified through liquid chromatography on a silica gel column (40–63  $\mu$ m; 1.0  $\times$  18 cm) using cyclohexane/acetone/chloroform 70:25:5 (v/v/v) as eluent.

\* Author to whom correspondence should be addressed (e-mail [ssortino@unict.it](mailto:ssortino@unict.it); fax 39 095-580138; telephone 39 095 7385062).

Xanthone was purchased from J. T. Baker Co. (Phillipsburg, NJ) and used as received. Anthracene and naphthalene were purchased from Sigma Chemical Co. (Milan, Italy) and used as received. All solvents used in the isolation of the photoproducts and in the photochemical experiments were of HPLC grade and were purchased from Lab-Scan (Dublin, Ireland).

**Instrumentation.** The absorption and fluorescence spectra were recorded with a Beckman DU 650 spectrophotometer and a Spex Fluorolog-2 (model F-111) spectrofluorometer, respectively. The fluorescence quantum yields were determined using naphthalene as a standard. The  $^1\text{H}$  NMR spectra were recorded on a Varian Inova spectrometer at 499.9 MHz and were obtained using tetramethylsilane (TMS) as internal reference.

An LC-ESI-MS system, equipped with an on-line photodiode array detector (DAD) and a LiChroCart RP-18 column (5  $\mu\text{m}$  packing, 4.6  $\times$  250 mm Hewlett-Packard), was used for analysis of the irradiated mixture. This was achieved by eluting in isocratic mode with a mixture of acetonitrile/water 60:40 (v/v) in 15 min, at a flow rate of 1 mL  $\text{min}^{-1}$ . The retention times of FN and its photoproducts were as follows: FN, 13.1 min; **1**, 3.6 min; **2**, 3.9 min; **3**, 1.8 min; **4**, 5.5 min; **5**, 6.8; **6**, 9.7 min.

**Nanosecond Laser Flash Photolysis.** The samples were excited with either the fourth (266 nm) or the third (355 nm) harmonic of a Nd:YAG. A Continuum Surelite II-10 laser system (pulse width = 6 ns fwhm) and the excited solution were analyzed at a right-angle geometry using a mini mLFP-111 apparatus developed by Luzchem Research. The monitoring beam was supplied by a ceramic xenon lamp and delivered through quartz fiber optical cables. The laser pulse was probed by a fiber that synchronized the mLFP system with a Tektronix TDS 3032 digitizer operating in the pretrigger mode. The signals from a compact Hamamatsu photomultiplier were initially captured by the digitizer and then transferred to a personal computer that controlled the experiments with Luzchem software developed, in the LabView 5.1 environment, from National Instruments. The energy of the laser pulse was measured at each laser shot by an SPHD25 Scientech pyroelectric energy monitor. The solutions for the experiments in the absence of oxygen were deoxygenated by bubbling with a vigorous and constant flux of pure argon (previously saturated with the solvent). In all experiments the solutions were renewed (in a flow cell of 1 cm optical path) after each laser shot. The sample temperature was 295  $\pm$  2 K.

**Irradiation Conditions.** The irradiation of FN was performed using a Rayonet photochemical reactor equipped with lamps emitting in the 280–320 nm range with a maximum at 300 nm. The incident photon flux on 3 mL quartz cuvettes was  $\sim 1 \times 10^{16}$  quanta  $\text{s}^{-1}$ . The experimental procedures of irradiation and the light intensity measurements have been described previously (11). On a preparative scale, the irradiation of FN was performed in a 200 mL quartz vessel. The steady-state experiments in the presence of xanthone were performed by irradiating the latter with “black light” phosphor lamps emitting in the 320–380 nm range with a maximum at 350 nm.

**Isolation and Characterization of the Photoproducts.** FN solutions (5  $\times 10^{-5}$  M) were irradiated in the Rayonet reactor under air-equilibrated solutions and continuous stirring. The irradiated solutions ( $\sim 30\%$  FN transformation, determined by LC-MS) were evaporated in vacuo at 60  $^\circ\text{C}$ . An analysis of the dried mixture was performed by thin-layer chromatography (TLC), on precoated silica gel 60 F254 plates (Merck) using cyclohexane/acetone/chloroform 70:25:5 (v/v/v) as eluent. On a preparative scale all of the photoproducts were obtained by liquid chromatography on a silica gel column (40–63  $\mu\text{m}$ ; 1.0  $\times$  18 cm) using cyclohexane/acetone/chloroform 70:25:5 (v/v/v) as eluent.

**O,O-Dimethyl O-[3-Methyl-4-(methylsulfinyl)phenyl]phosphorothioate (1):**  $^1\text{H}$  NMR (500 MHz,  $\text{CDCl}_3$ , TMS)  $\delta$  7.86 (d,  $J = 8.5$  Hz, 1H, Ph), 7.29 (d,  $J = 8.2$  Hz, 1H, Ph), 7.12 (s, 1H, Ph), 3.87 (d,  $J = 13.99$  Hz from P, 6H,  $\text{OCH}_3$ ), 2.77 (s, 3H,  $\text{SCH}_3$ ), 2.42 (s, 3H,  $\text{PhCH}_3$ ); ESI-MS,  $m/z$  295  $[\text{M} + \text{H}]^+$ ; UV-vis (MeOH)  $\lambda_{\text{max}} = 236$  nm ( $\epsilon = 7.800 \text{ M}^{-1} \text{ cm}^{-1}$ ), 275 nm ( $\epsilon = 1.000 \text{ M}^{-1} \text{ cm}^{-1}$ ).

**3-Methyl-4-(methylthio)phenol (2):**  $^1\text{H}$  NMR (500 MHz,  $\text{CDCl}_3$ , TMS)  $\delta$  7.15 (d,  $J = 8.4$  Hz, 1H, Ph), 6.65 (d,  $J = 8.4$  Hz, 1H, Ph), 6.61 (m, 1H, Ph), 4.6 (s, 1H, OH), 2.44 (s, 3H,  $\text{SCH}_3$ ), 2.30 (s, 3H,

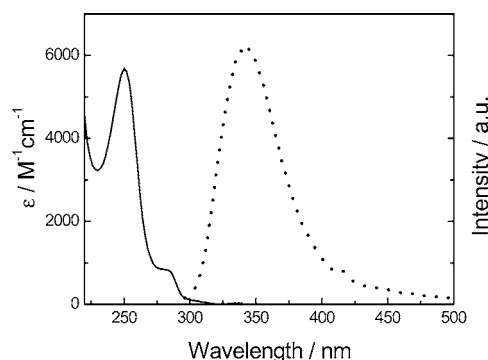


**Figure 1.** Absorption (—) and fluorescence (---) spectra of FN in aqueous solution.

$\text{PhCH}_3$ ); ESI-MS,  $m/z$  153  $[\text{M} - \text{H}]^-$ ; UV-vis (MeOH)  $\lambda_{\text{max}} = 245$  nm ( $\epsilon = 4.700 \text{ M}^{-1} \text{ cm}^{-1}$ ), 291 nm ( $\epsilon = 860 \text{ M}^{-1} \text{ cm}^{-1}$ ).

**3-Methyl-4-(methylsulfinyl)phenol (3):**  $^1\text{H}$  NMR (500 MHz,  $\text{CDCl}_3$ , TMS)  $\delta$  7.36 (d,  $J = 8.4$  Hz, 1H, Ph), 6.76 (s, 1H, Ph), 6.73 (m,  $J = 8.4$  Hz, 1H, Ph), 4.6 (s, 1H, OH), 2.77 (s, 3H,  $\text{SCH}_3$ ), 2.42 (s, 3H,  $\text{PhCH}_3$ ); ESI-MS,  $m/z$  169  $[\text{M} - \text{H}]^-$ ; UV-vis (MeOH)  $\lambda_{\text{max}} = 230$  nm ( $\epsilon = 4.500 \text{ M}^{-1} \text{ cm}^{-1}$ ), 275 nm ( $\epsilon = 1000 \text{ M}^{-1} \text{ cm}^{-1}$ ).

**O,O-Dimethyl S-[3-Methyl-4-(methylthio)phenyl]phosphorothioate (4):**  $^1\text{H}$  NMR (500 MHz,  $\text{CDCl}_3$ , TMS)  $\delta$  7.41 (d,  $J = 8.5$  Hz, 1H, Ph), 7.35 (s, 1H, Ph), 7.22 (d,  $J = 8.5$  Hz, 1H, Ph), 3.83 (d,  $J = 12.99$  Hz from P, 6H,  $\text{OCH}_3$ ), 2.49 (s, 3H,  $\text{SCH}_3$ ), 2.29 (s, 3H,  $\text{PhCH}_3$ ); ESI-MS,  $m/z$  279  $[\text{M} + \text{H}]^+$ ; UV-vis (MeOH)  $\lambda_{\text{max}} = 264$  nm ( $\epsilon = 4.100 \text{ M}^{-1} \text{ cm}^{-1}$ ).

**4-Chloro-2-methylphenyl(methyl)sulfane (5):**  $^1\text{H}$  NMR (500 MHz,  $\text{CD}_3\text{CN}$ , TMS)  $\delta$  7.16 (d,  $J = 8.5$  Hz, 1, Ph), 6.99 (d,  $J = 8.0$  Hz, 1H, Ph), 6.70 (m, 1H, Ph), 2.36 (s, 3H,  $\text{SCH}_3$ ), 2.30 (s, 3H,  $\text{PhCH}_3$ ); ESI-MS,  $m/z$  173.5  $[\text{M} + \text{H}]^+$ .

**4-Methoxy-2-methylphenyl(methyl)sulfane (6):**  $^1\text{H}$  NMR (500 MHz,  $\text{CDCl}_3$ , TMS)  $\delta$  7.25 (d,  $J = 8.5$  Hz, 1H, Ph), 6.75 (d,  $J = 8.5$  Hz, 1H, Ph), 6.72 (m, 1H, Ph), 3.73 (s, 3H,  $\text{OCH}_3$ ), 2.44 (s, 3H,  $\text{SCH}_3$ ), 2.33 (s, 3H,  $\text{PhCH}_3$ ); ESI-MS,  $m/z$  169  $[\text{M} + \text{H}]^+$ .

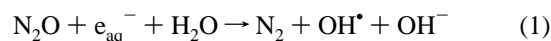
## RESULTS

**Absorption and Emission.** The absorption spectrum of FN in aqueous solution is characterized by a main band peak at 250 nm, a shoulder at  $\sim 285$  nm, and a tail extending to 320 nm (Figure 1). The fluorescence emission exhibits an intense and unstructured band with a maximum at 342 nm. On the basis of the small overlap of the fluorescence emission with the lowest energy absorption band, the lowest excited singlet state can be experimentally located at  $\sim 390$  kJ/mol.

The fluorescence quantum yield in water is found to be  $\Phi_f = 0.06$ . This value decreases only slightly in less polar solvents such as acetonitrile or methanol. In contrast, the emission maximum exhibits significant blue shifts of 12 and 16 nm in acetonitrile and methanol, respectively.

**Laser Flash Photolysis Studies.** Figure 2 shows the transient absorption spectra of FN recorded in aqueous solution 0.1  $\mu\text{s}$  after a 266 nm laser pulse, under different experimental conditions.

The spectrum recorded in Ar-saturated solutions is characterized by a maximum at 320 nm and a broad absorption extending beyond 700 nm. The virtually complete disappearance of this absorption, with the consequent appearance of a better defined band with a maximum at  $\sim 540$  nm, is observed when the spectrum is recorded in  $\text{N}_2\text{O}$ -saturated solutions. As is well-known,  $\text{N}_2\text{O}$  is a powerful electron scavenger ( $k_q = 9.1 \times 10^9 \text{ M}^{-1} \text{ s}^{-1}$ ) (12) and in few nanoseconds converts the solvated electrons ( $e_{\text{aq}}^-$ ) according to eq 1:



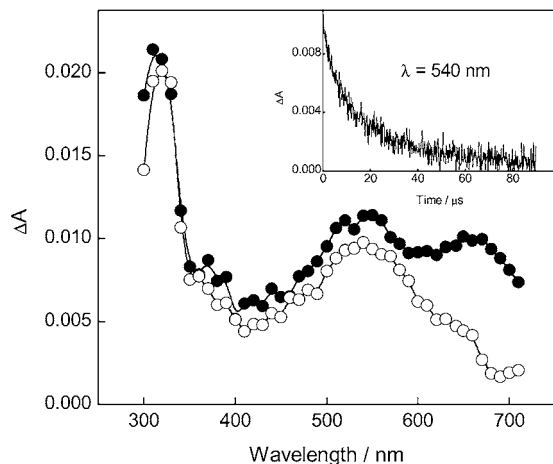


**Figure 2.** Transient absorption spectra observed upon 266 nm laser excitation of  $1 \times 10^{-4}$  M aqueous solution of FN, 0.1  $\mu$ s after the pulse in (●) Ar-saturated solution or in (○)  $N_2O$ -saturated solution. (Inset) Decay trace observed at 540 nm in  $N_2O$ -saturated solution.  $E_{266} \sim 8$  mJ/pulse. Each point was obtained by signal average of 15 traces.

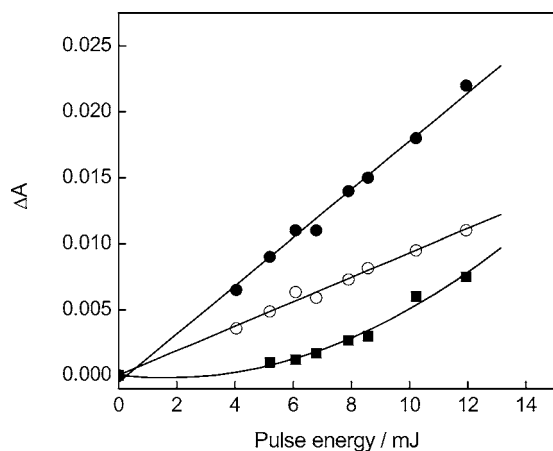


**Figure 3.** Laser intensity dependence of the absorbance changes, taken 0.1  $\mu$ s after pulse, observed upon 266 nm laser excitation of  $1 \times 10^{-4}$  M aqueous solution of FN at (●) 320 and (○) 540 nm in  $N_2O$ -saturated solution and at (■) 720 nm in Ar-saturated solution. Each point was obtained by signal average of 15 traces.

This result clearly indicates that photoionization occurs in the laser photolysis of FN.

The decay profiles at both 540 (see inset of **Figure 2**) and 320 nm recorded in  $N_2O$ -saturated solutions are fitted fairly well by a monoexponential analysis that affords the same rate constant of  $6 \times 10^4$   $s^{-1}$  (note that the decay becomes faster and involves a second-order component at increasing intensity of the excitation laser pulse). Therefore, it is safe to assign these absorption maxima to the same transient species. Moreover, no relevant new bands are observed concurrently to its decay, as suggested by the difference absorption spectra recorded with elapsing time.

To determine if the photoionization and the formation the 320–540 nm transient are interrelated processes, the laser intensity dependence of the initial absorbance at 720 nm (maximum of the hydrated electrons), 540, and 320 nm was inspected. To exclude any contribution of  $e_{aq}^-$  to the absorbance monitored at 320 and 540 nm, the laser intensity effect at these wavelengths was examined in  $N_2O$ -saturated solution. **Figure 3** shows a linear dependence of the 320–540 nm transient on the pulse energy, according to a monophotonic process. On the other hand, the  $e_{aq}^-$  data are fitted well by a second-order polynomial,

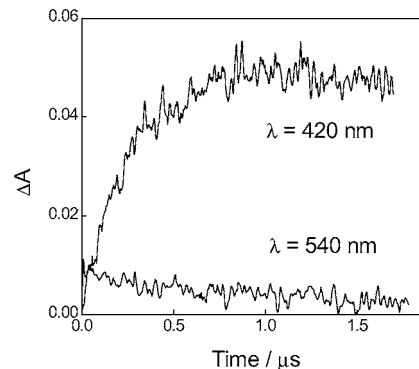


**Figure 4.** Absorption time profiles observed upon 266 nm laser excitation of Ar-saturated methanol solution of FN in the presence of  $8 \times 10^{-5}$  M AN at 540 nm (decay) and 420 nm (buildup). For the sake of clarity, the initial “instantaneous” absorption at 420 nm due to the direct generation of the AN triplet has been subtracted.

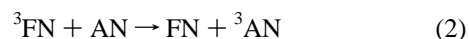
suggesting that electron photoejection mainly occurs via a two-photon mechanism.

On the basis of the above results it can be concluded that the two photoprocesses are parallel and unrelated because if the 540–320 nm transient was generated in a reaction initiated by prior photoionization, the same trend at the explored wavelengths would have been expected.

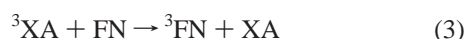
The active role played by singlet oxygen in the FN photolysis (9) (see the Introduction) besides the lifetime of the 320–540 nm transient in the microsecond time scale led us to suspect this transient as the lowest excited triplet state of FN. To substantiate this hypothesis we designed appropriate experiments in the presence of either anthracene (AN) or xanthone (XA). These compounds are characterized by low and high triplet energy, respectively ( $E_T$  AN  $\sim 167$   $kJ\ mol^{-1}$ ,  $E_T$  XA  $\sim 314$   $kJ\ mol^{-1}$ ), and offer the advantage of possessing well-known triplet–triplet (T–T) absorption spectra with maxima,  $\sim 420$  nm for AN and  $\sim 600$  nm for XA (13), not superimposed to the 320–540 nm transient. Due to the low solubility of AN and XA in water, the above measurements were carried out in methanol solution. Control experiments carried out in this solvent with FN alone showed no significant changes either in the absorption maxima or in the lifetime of the transient photogenerated, if compared with aqueous solution.

**Figure 4** shows the time profiles monitored at two key wavelengths when an Ar-saturated methanol solution of FN is excited with a 266 nm pulse in the presence of  $8 \times 10^{-5}$  M AN. Under these experimental conditions the decay of the 540 nm transient is monoexponential and characterized by a rate constant almost 1 order of magnitude larger than that observed in the absence of AN. The signal at 420 nm shows an intense “instantaneous” absorption, due to the direct generation of the AN triplet, and thereafter a further buildup of the absorbance. The instantaneous absorption is not surprising, considering that a fraction of the incident photons ( $\sim 10\%$ ) is also absorbed by AN under our experimental conditions. For the sake of clarity, the trace at 420 nm reported in **Figure 4** is subtracted by this fast initial absorption.

Interestingly, the pseudo-first-order analysis of the growth trace matches well the decay at 540 nm. These results corroborate the assignment of the 540 nm transient to the lowest triplet state of FN, being in accordance with the following energy transfer process:



In a complementary experiment, an Ar-saturated methanol solution of XA was excited with a 355 nm laser pulse in the presence of  $10^{-3}$  M FN. This excitation source offers the advantage of precluding any direct excitation by FN, allowing the selective excitation of XA. **Figure 5** shows the transient absorption spectra recorded at different delay times with respect to the laser pulse. The spectrum taken at 0.1  $\mu$ s shows two bands with maxima at 580 and 300 nm, respectively, according to the typical spectral features of the lowest triplet state of XA in polar solvent (14). The decrease of the XA triplet with elapsing time is accompanied by the concomitant formation of a new transient species with maxima at ca. 320 and 540 nm. These spectral features are very similar to those observed by direct excitation of FN reported in **Figure 2** (the slightly different ratio of the UV and visible bands may be due to the ground-state absorption of XA in the UV region) and well agree with the photosensitization of the FN triplet through the following energy transfer process:



The decay at 580 nm and the growth at 320 nm were also monitored at different concentrations of FN in the range from  $10^{-3}$  to  $2 \times 10^{-4}$  M. The straight line of the linear plots  $k_{\text{obs}}$  versus [FN] yielded, for the above reaction, a diffusion-controlled bimolecular quenching constant,  $k_q = 7.5 \times 10^9 \text{ M}^{-1} \text{ s}^{-1}$ . The experiment reported in **Figure 5** also allows the extinction coefficient of the FN triplet to be determined. Considering that the fraction of the XA triplet quenched by FN in this experiment is >95%, a value of  $\sim 3500 \text{ M}^{-1} \text{ cm}^{-1}$  for  $\Delta\epsilon$  at 540 nm is calculated by eq 4

$$\Delta A({}^3\text{FN}_{540}) \times \Delta\epsilon({}^3\text{XA}_{580}) = \Delta A({}^3\text{XA}_{580}) \times \Delta\epsilon({}^3\text{FN}_{540}) \quad (4)$$

where the  $\Delta A$  values refer to the absorbance of the XA triplet at the beginning (0.1  $\mu$ s after the laser pulse) and the FN triplet at the end (1  $\mu$ s after the laser pulse) of reaction 3, respectively (13). An average value of 6800 was used for  $\Delta\epsilon({}^3\text{XA}_{580})$  (13).

The intersystem-crossing quantum yield ( $\Phi_{\text{isc}}$ ) of FN in water was calculated by the comparative method using a solution of naphthalene (NP) in acetonitrile with the same absorbance (0.2). Thus,  $\Phi_{\text{isc}}$  was obtained by application of eq 5

$$\Phi_{\text{isc}}(\text{FN}) = \Phi_{\text{isc}}(\text{NA}) \times \pi({}^3\text{FN}) \times \Delta\epsilon_{440}({}^3\text{NA})/\pi({}^3\text{NA}) \times \Delta\epsilon_{540}({}^3\text{FN}) \quad (5)$$

where the  $\pi$  values refer to the slopes of the linear plot representing the absorbance of the FN triplet state in water at 540 nm and the NA triplet in acetonitrile at 440 nm as a function of the pulse energy. Using the values of ca. 3500 (determined above) for  $\Delta\epsilon_{540}$  of FN, 9600 for  $\Delta\epsilon_{440}({}^3\text{FN})$ <sup>13</sup>, and 0.28 for  $\Phi_{\text{isc}}(\text{NA})$ <sup>13</sup>, a  $\Phi_{\text{isc}}(\text{FN})$  of  $\sim 0.3$  is obtained.

**Steady-State Photolysis.** The photoproducts obtained after irradiation with 300 nm light of aqueous solutions of  $10^{-4}$  M FN in different experimental conditions are shown in **Scheme 1**. In air-equilibrated solutions four main photoproducts, **1–4**, are observed. Three of them, **1–3**, were also recently identified by Hirahara et al. (9, 10), whereas the remaining product, **4**, was never detected before.

As reasonably expected, the oxidation products **1** and **3** are formed only in traces when FN photolysis is carried out in Ar-saturated aqueous solutions, whereas, in contrast, **2** and **4** are the major products observed. The formation of such photoproducts is totally inhibited when FN is irradiated in the presence

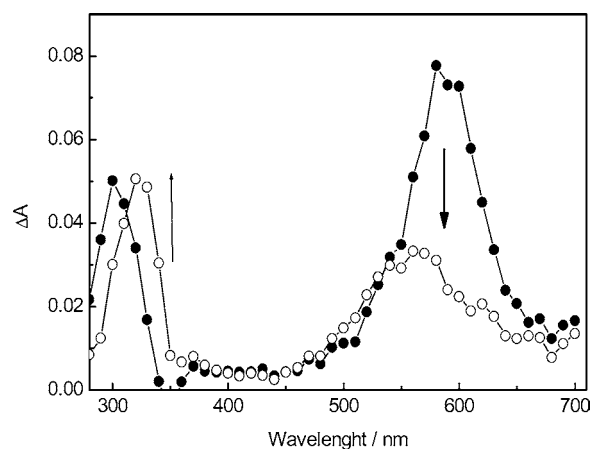


**Figure 5.** Transient absorption spectra observed upon 355 nm laser excitation of Ar-saturated methanol solution of  $1 \times 10^{-4}$  M XA in the presence of  $10^{-3}$  M FN, 0.1 (●) and 1  $\mu$ s (○) after pulse. Each point was obtained by signal average of 10 traces.

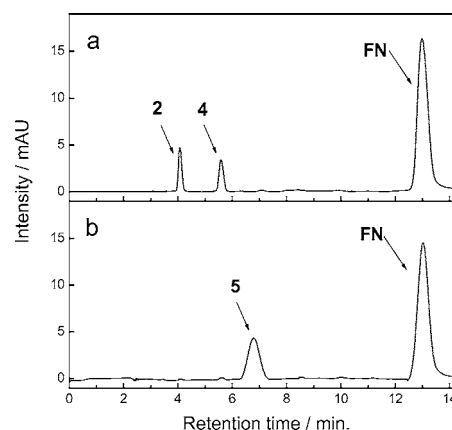


**Figure 6.** HPLC chromatogram of photodegradation observed after FN photolysis in aqueous Ar-saturated solution (a) in the absence and (b) in the presence of 0.1 M  $\text{Cl}^-$ . DAD wavelength = 254 nm.

of 0.1 M  $\text{Cl}^-$ , and besides a new peak is detected by HPLC (**Figure 6**). Under these experimental conditions, the only stable photoproduct is identified as the chloro derivative **5**.

Further insights into FN photodegradation were obtained by irradiating the pesticide in neat methanol in the absence of oxygen. Under these conditions, product **4** is accompanied by the formation of the alkoxy derivative **6** in the place of the phenol derivative **2**.

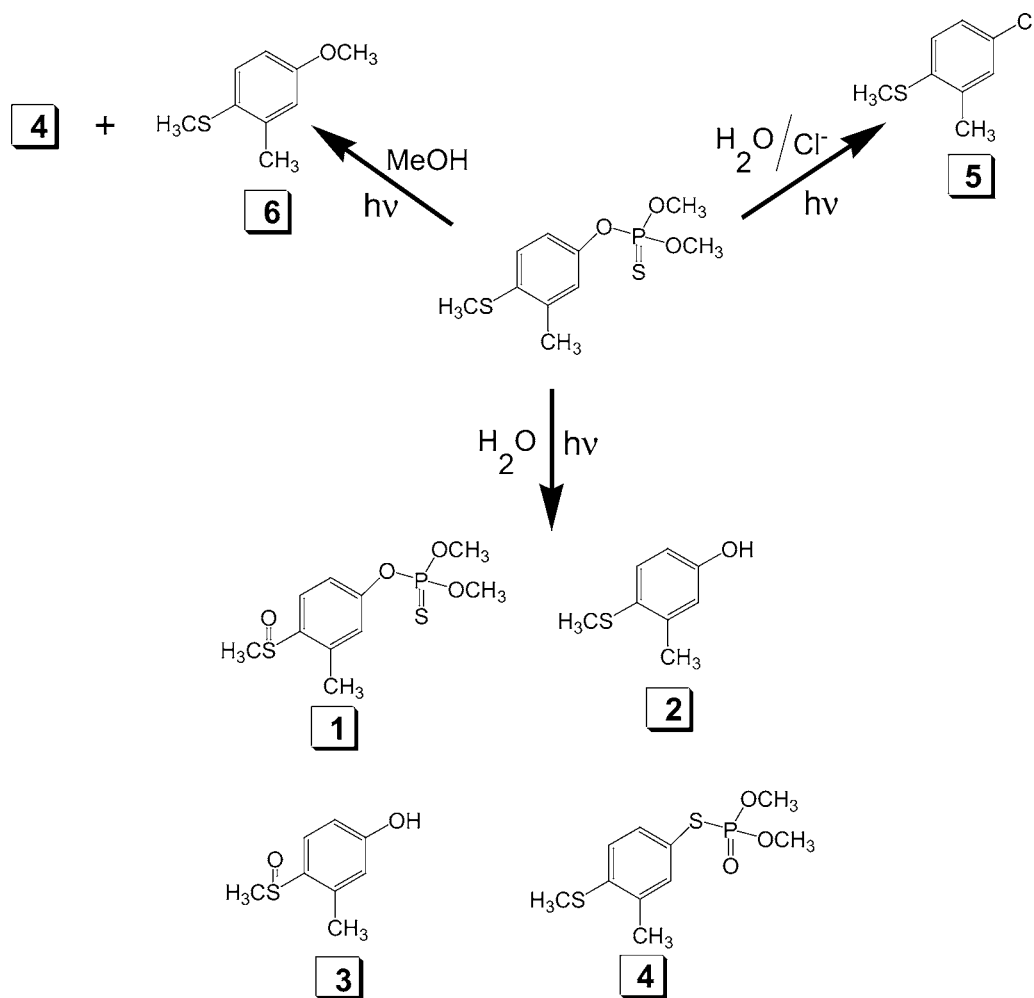
The influence of a triplet photosensitizer, such as XA, on the photodegradation of FN was also evaluated. In this regard, an Ar-saturated methanol solution of XA was excited with 350 nm light in the presence of  $10^{-3}$  M FN. This excitation source precludes any direct excitation of FN, allowing the selective excitation of XA. Moreover, the concentration of FN used was high enough to ensure the almost complete quenching of the XA triplet, leading to the photosensitized formation of the FN triplet (see Laser Flash Photolysis Studies). However, the HPLC analysis of the irradiated mixture does not reveal any FN photodecomposition, even after prolonged irradiation times.

## DISCUSSION

The above results provide interesting insights into the photoreactivity of the organophosphorus pesticide FN and shed more light onto its photodegradation mechanism.

Two main transient intermediates are detected upon laser excitation of aqueous solutions of FN, the lowest excited triplet

Scheme 1



state and hydrated electrons (15). The laser intensity dependence of these species clearly highlights their different natures. Although, as expected, the triplet is generated through a monophotonic process, a biphotonic pathway is responsible for the photoionization (Figure 3). In general, two-photon processes are unimportant under typical environmental conditions (i.e., steady-state illumination) due to the low light intensity level of irradiation. Therefore, it is conceivable to infer that the photoionization plays only a negligible role in the photodegradation of the pesticide. This finding is in accordance with a foregoing steady-state photochemical study that ruled out the participation of active oxygen radical species such as hydroxyl and superoxide radicals in the FN photolysis (9). Actually, generation of hydrated electrons under steady-state irradiation conditions would have led to the above oxygen radicals as a consequence of fast ( $k_q = 1.9 \times 10^{10} \text{ M}^{-1} \text{ s}^{-1}$ ) reaction with molecular oxygen (12).

Of the four stable photoproducts isolated in neat water (see Scheme 1) 4 was never observed before. Such a product, together with the phenol derivative 2, is formed independently by the presence of oxygen. With regard to the excited state triggering the formation of such products (2 and 4), the combination of time-resolved and steady-state experiments, carried out in the presence of XA, provides an important clue. In fact, the observation that the selective excitation of XA populates the FN triplet via an efficient energy transfer process (see Figure 5), but does not lead to the concurrent degradation of the pesticide, rules out the participation of the lowest triplet

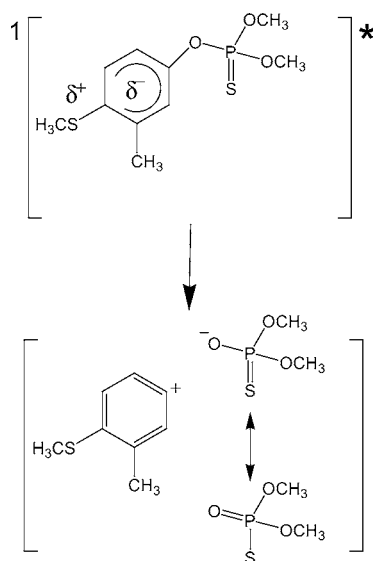
state of FN. Therefore, formation of these products seems to be more likely triggered by a short-lived excited singlet state.

As mentioned in the Introduction, photohydrolysis involving a nucleophilic attack of water molecules to the P atom and subsequent heterocleavage of the O–P bond has been proposed as one of the main primary processes occurring upon light absorption (9). In this context it should be noted that although the above mechanism may explain the formation of the phenol derivative 2, it cannot account for the formation of 4. In fact, generation of the latter should imply the formal Ar–O bond cleavage and subsequent formation of the Ar–S bond. Therefore, the observation of the new product 4 opens a new issue concerning the primary photoreaction pathways.

The mechanism proposed is shown in Scheme 2 and may account for the formation of both photoproducts 2 and 4. It involves the lowest excited singlet state of the pesticide and a “ $\sigma$  aryl cation” as the key intermediate into the FN photodecomposition.

We believe that the reactivity of the singlet state might be related to its internal charge transfer character most likely due to the presence of the electron-donating  $\text{CH}_3\text{—S}$  substituent. This character is indicated by the Stokes shift between the absorption and emission maxima (see Figure 1) and is in agreement with the red shift of the fluorescence maximum with increasing solvent polarity. On these grounds, the proposed initiating photochemical step involves a fast heterolytic fragmentation of the Ar–O bond, before isc, with consequent formation of a  $\sigma$  aryl cation and release of the side chain. Although laser flash

Scheme 2



photolysis measurements do not provide any direct evidence for the formation of this intermediate, this is not surprising and may be strictly related to the *singlet* nature of the aryl cation. Actually, *singlet* aryl cations, photogenerated by similar and even more conjugated chromophores than FN, are reported to be short-lived, exhibiting only weak absorption in the whole range of wavelengths explored (16).

However, a strong piece of evidence for the photogeneration of the proposed aryl cation is given by the observation of the chloro derivative **5** and the alkoxy derivative **6** when the photolysis is carried out in a chloride-containing aqueous solution and in methanol solution, respectively (see **Scheme 1**). Beyond validating the occurrence of the Ar–O bond heterocleavage, the fact that both chloride and methanol trap the cation represents further support of the proposed *singlet* nature of this transient species. Actually, *singlet* cations are known to react with “ $\sigma$  nucleophiles” such as chloride and methanol (or water) (17–20), in contrast to *triplet* cations photogenerated from triplet states, which show a remarkable preference for “ $\pi$ -type nucleophiles” (17–20). In this view, the formation of photoproducts **2** and **4** may be interpreted on the basis of two competitive pathways taking place after the Ar–O bond heterocleavage and involving nucleophilic attack to the photogenerated aryl cation by either water molecules (leading to **2**) or the sulfur atom of the leaving side chain (leading to **4**).

As far as the photo-oxidation products **1** and **3** are concerned, the effective population of the FN triplet ( $\Phi_{isc} \sim 0.3$ ) and its long lifetime ( $\sim 16 \mu s$ ) are in excellent agreement with the recent studies of Hirahara et al., who demonstrated the direct involvement of  $O_2$  ( $^1\Delta_g$ ) in the formation of the above oxidation products by using rose bengal as  $O_2$  ( $^1\Delta_g$ ) photosensitizer (9).

In conclusion, the present investigation sheds more light on the primary photoprocesses of the organophosphorus pesticide FN. The obtained results may be of both photochemical and photobiological significance. With regard to the former aspect, the most striking outcome of this study is the participation of an aryl cation in the FN photodecomposition. The accessibility to these species in solution is, in fact, quite difficult, as witnessed by the limited number of cases reported to date (17–21). According to the literature, the *singlet* nature of the aryl cation is reflected in its reactivity toward “ $\sigma$  nucleophiles” as well as in its optical transparency in the UV–vis spectral region. Therefore, these results, besides providing a novel contribution

to the general topic of photoinitiated reactions of pesticide compounds, may add to the understanding of the still poorly known chemical behavior of aryl cations.

As far as the photobiological interest of the present work is concerned, it should be stressed that in addition to the predictable toxic effects related to the potential of FN to be ingested by humans with agriculture products, “phototoxic” phenomena might also be involved. In this concern, the triplet state, the aryl cation, or both can have a potential role. Actually, the former species may induce phototoxicity via typical “type II” photoprocesses (22), and the aryl cation may react with biological sites through “covalent binding”. Similar photoreactions have recently been proposed at the origin of the phototoxic and photocarcinogenic effects induced by drugs photogenerating aryl cations (23).

#### ACKNOWLEDGMENT

We thank Profs. G. Condorelli and L. L. Costanzo for their support.

#### LITERATURE CITED

- (1) Racke, K. D. Degradation of organophosphorus insecticides in environmental matrices. In *Organophosphates: Chemistry, Fate, and Effects*; Chambers, J. E., Levy, P. Z., Eds; Academic Press: San Diego, CA, 1992; pp 48–78.
- (2) Aly, O. A.; Badawy, M. I. Hydrolysis of organophosphates insecticides in aqueous media. *Environ. Int.* **1982**, *7*, 373–377.
- (3) Minelli, E. V.; Cabras, P.; Angioni, A.; Garau, V. L.; Mekis, M.; Pirisi, F. M.; Cabitza, F.; Cubeddu, M. Persistence and metabolism of fenthion in orange fruit. *J. Agric. Food Chem.* **1996**, *44*, 936–939.
- (4) Cabras, P.; Garau, V. L.; Melis, M.; Pirisi, F. M.; Spanedda, L. Persistence and fate of fenthion in olives and olive products. *J. Agric. Food Chem.* **1993**, *41*, 2431–2433.
- (5) Nomeir, A. A.; Hajjar, N. P. Metabolism of chlordane in mammals. *Environ. Contam. Toxicol.* **1987**, *100*, 1–22.
- (6) Robinson, D. E.; Mansingh, A.; Dasgupta, T. P. Fate and transport of ethoprophos in the Jamaican environment. *Sci. Total Environ.* **1999**, *30*, 373–379.
- (7) See, for example: Draper, W. M.; Crosby, D. G. Solar photooxidation of pesticides in dilute hydrogen peroxide. *J. Agric. Food Chem.* **1984**, *32*, 231–237. Crosby, D. G.; Moilanen, K. W.; Nakagawa, M.; Wong, A. S. Photonucleic reactions of pesticides. *Environmental Toxicology of Pesticides*; Academic Press: New York, 1972; pp 423–433. Chukwudebe, A.; March, R. B.; Othman, M.; Fukuto, T. R. Formation of trialkyl phosphorothioate esters from organophosphorus insecticides after exposure to either ultraviolet light or sunlight. *J. Agric. Food Chem.* **1989**, *37*, 539–545. Katagi, T. Photochemistry of organophosphorus herbicide butamifos. *J. Agric. Food Chem.* **1993**, *41*, 496–501; Konstantinou, I. K.; Albanis, T. A. Photocatalytic transformation of pesticides in aqueous titanium dioxide suspensions using artificial and solar light: intermediates and degradation pathways. *Appl. Catal. B: Environ.* **2003**, *42*, 319–335.
- (8) Hirahara, Y.; Sayato, Y.; Nakamuro, K. Study on photochemical behavior of pesticides in the environment. *Jpn. J. Toxicol. Environ. Health* **1998**, *44*, 451–461.
- (9) Hirahara, T.; Ueno, H.; Nakamuro, K. Aqueous photodegradation of fenthion by ultraviolet B irradiation: contribution of singlet oxygen in photodegradation and photochemical hydrolysis. *Water Res.* **2003**, *37*, 468–476.
- (10) Hirahara, T.; Ueno, H.; Nakamuro, K. Comparative photodegradation study of Fenthion and disulfoton under irradiation of different light sources in liquid- and solid-phase. *Jpn. J. Toxicol. Environ. Health* **2001**, *47*, 129–135.

- (11) De Guidi, G.; Chillemi, R.; Costanzo, L. L.; Giuffrida, S.; Sortino, S.; Condorelli, G. Molecular mechanism of drug photosensitization 5. Photohemolysis sensitized by Suprofen. *J. Photochem. Photobiol. B: Biol.* **1994**, *23*, 125–133.
- (12) Buxton, G. V.; Greenstock, C. L.; Helman, W. P.; Ross, A. B. *J. Phys. Chem. Ref. Data* **1998**, *17*, 513.
- (13) Carmichael, I.; Hug, G. L. Triplet–triplet absorption spectra of organic molecules in condensed phases. *J. Phys. Chem. Ref. Data* **1986**, *15*, 1–250.
- (14) Scaiano, J. C. Solvent effects in the photochemistry of xanthone. *J. Am. Chem. Soc.* **1980**, *102*, 7747–7753.
- (15) Although the photoionization event necessarily leaves a radical cation, we did not have any spectral evidence for this species. The low extinction coefficient and/or the low photoproduction quantum yield of this species could be two potential reasons precluding its detection.
- (16) See, for example: (a) Gasper, S. M.; Devadoss, C.; Shuster, G. B. Photolysis of substituted benzenediazonium salts: spin-selective reactivity of aryl cations. *J. Am. Chem. Soc.* **1995**, *117*, 5206–5211. (b) Monti, S.; Sortino, S.; Fasani, E.; Albini, A. Multifaceted photoreactivity of 6-fluoro-7-aminoquinolones from the lowest excited states in aqueous media: a study by nanosecond and picosecond spectroscopic techniques. *Chem. Eur. J.* **2001**, *7*, 2185–2196.
- (17) Stang, P. J. Alkynyl and aryl cations. In *Dicoordinate Carbocations*; Rappoport, Z., Stang, P. J., Eds.; Wiley: New York, 1997; pp 451–460.
- (18) Guizzardi, B.; Mella, M.; Fagnoni, M.; Freccero, M.; Albini, A. Generation and reactivity of the 4-aminophenyl cation by photolysis of 4-chloroaniline. *J. Org. Chem. Soc.* **2001**, *66*, 6353–6363 and references cited therein.
- (19) Mella, M.; Esposti, S.; Fagnoni, M.; Albini, A. A novel access to 3-aryl-2-norbornyl cation. *Chem. Commun.* **2003**, 738–739.
- (20) Steenken, S.; Askokkuna, M.; Maruthamuthu, P.; McClelland, R. A. Making photochemically generated phenyl cations visible by addition to aromatics: production of phenylcyclohexadienyl cations and their reactions with bases/nucleophiles. *J. Am. Chem. Soc.* **1998**, *120*, 11925–11931.
- (21) Mella, M.; Fagnoni, M.; Freccero, M.; Fasani, E.; Albini, A. New synthetic methods via radical cation fragmentation. *Chem. Soc. Rev.* **1998**, *27*, 81–89.
- (22) *Handbook of Organic Photochemistry and Photobiology*; Horspool, W. M., Song, P. S., Eds.; CRC: Boca Raton, FL, 1995.
- (23) Albini, A.; Monti, S. Photophysics and photochemistry of fluoroquinolones. *Chem. Soc. Rev.* **2003**, *32*, 238–250.

---

Received for review March 22, 2004. Revised manuscript received July 17, 2004. Accepted July 19, 2004. Financial support from MIUR “Cofinanziamento di Programmi di Ricerca di Rilevante Interesse Nazionale” and INCA (Consorzio Interuniversitario per la Chimica dell’Ambiente) is gratefully acknowledged.

JF049539X